DOI: 10.1534/genetics.107.082503

A *Mutator* Transposon Insertion Is Associated With Ectopic Expression of a Tandemly Repeated Multicopy *Myb* Gene *pericarp color1* of Maize

Michael L. Robbins,* Rajandeep S. Sekhon,* Robert Meeley† and Surinder Chopra*,[1]

**Department of Crop and Soil Sciences, Pennsylvania State University, University Park, Pennsylvania 16802 and* †*Pioneer—A DuPont Company, Johnston, Iowa 50131*

Manuscript received September 26, 2007
Accepted for publication January 28, 2008

ABSTRACT

The molecular basis of tissue-specific pigmentation of maize carrying a tandemly repeated multicopy allele of *pericarp color1* (*p1*) was examined using *Mutator* (*Mu*) transposon-mediated mutagenesis. The *P1-wr* allele conditions a white or colorless pericarp and a red cob glumes phenotype. However, a *Mu*-insertion allele, designated as *P1-wr-mum6*, displayed an altered phenotype that was first noted as occasional red stripes on pericarp tissue. This gain-of-pericarp-pigmentation phenotype was heritable, yielding families that displayed variable penetrance and expressivity. In one fully penetrant family, deep red pericarp pigmentation was observed. Several reports on *Mu* suppressible alleles have shown that *Mu* transposons can affect gene expression by mechanisms that depend on transposase activity. Conversely, the *P1-wr-mum6* phenotype is not affected by transposase activity. The increased pigmentation was associated with elevated mRNA expression of *P1-wr-mum6* copy (or copies) that was uninterrupted by the transposons. Genomic bisulfite sequencing analysis showed that the elevated expression was associated with hypomethylation of a floral-specific enhancer that is ~4.7 kb upstream of the *Mu1* insertion site and may be proximal to an adjacent repeated copy. We propose that the *Mu1* insertion interferes with the DNA methylation and related chromatin packaging of *P1-wr*, thereby inducing expression from gene copy (or copies) that is otherwise suppressed.

WHOLE-genome amplification and tandem duplication events are the two chief mechanisms for the evolution of gene families in plants (Rizzon *et al.* 2006). Following duplication, many redundant genes are deleted or become pseudogenes; however, some genes have evolved specialized functions in the regulation of transcription, signal transduction, and development (Blanc *et al.* 2003; Maere *et al.* 2005). Tandem duplications are widespread among genes that have roles in disease resistance and the synthesis of secondary metabolites (Hulbert and Bennetzen 1991; Kliebenstein *et al.* 2001). Tandemly arranged gene copies often have specialized biological roles that may have contributed to their conservation. For example, Botrytis disease is combated in Arabidopsis by two tandemly arranged genes that encode polygalacturonase-inhibiting proteins (Ferrari *et al.* 2003). Both the gene copies have similar protein products but have diverged in regulatory regions so that they are activated by separate signal transduction pathways. Developmental processes can also be tightly regulated on the basis of the differential activation of gene copies. For instance, the demand for the patatin storage protein during potato tuberization is met by preferentially upregulating a subset of copies from an ~10- to 18-copy locus (Stupar *et al.* 2006).

Tandem duplication can both positively and negatively affect gene expression. In barley, the resistance to powdery mildew is associated with a tandem duplication in the *Mlo* gene that encodes a seven-transmembrane domain protein (Piffanelli *et al.* 2004). In this case, an additional truncated copy functions to block the expression of wild-type transcripts. Conversely, a tandem duplication of the maize homeobox gene called *knotted1* (*kn1*) has given rise to a mutant allele, *Kn1-O*, which is ectopically expressed in leaves (Veit *et al.* 1990; Vollbrecht *et al.* 1991). Aberrant expression in *kn1* mutants can easily be monitored by the presence of knots that are composed of displaced ligule tissue (Smith *et al.* 1992). Derivative alleles of *Kn1-O* indicate that the presence of a third copy increases the severity of the phenotype, whereas the loss of a copy results in the restoration of wild-type function (Veit *et al.* 1990). Moreover, insertion of *Mu* transposons at the junction of the *Kn1-O* repeat restores the wild-type expression pattern (Lowe *et al.* 1992).

These studies indicate that gene copies have evolved important biological functions and can thus profoundly affect gene expression. Despite this, tandem arrays of genes encoding for transcription factors are infrequent, theoretically because of the deleterious nature of gene

Sequence data from this article have been deposited with the EMBL/GenBank Data Libraries under accession nos. EU137661–EU137662.

[1]*Corresponding author:* 116 Agricultural Science and Industries Bldg., Pennsylvania State University, University Park, PA 16802.
E-mail: sic3@psu.edu

rearrangements (Rizzon *et al.* 2006). However, the presence of tandem repeats in regulatory genes should have a broader effect on the regulation of biosynthetic pathways. Herein, we have focused on a well-studied maize transcription factor called *pericarp color1* (*p1*), which has numerous alleles that differ with respect to their copy number (Cocciolone *et al.* 2001). The *p1* gene encodes a *myb*-homologous protein that regulates the transcription of structural genes required for the biosynthesis of brick-red flavonoid pigments called phlobaphenes (Grotewold *et al.* 1994). The tissue specificity of phlobaphene pigmentation on maize ears depends upon the allelic constitution at the *p* locus. Stable alleles of the *p1* gene have been named according to their pericarp and cob pigmentation phenotypes: *P1-wr* (white pericarp, red cob), *P1-rr* (red pericarp, red cob), *P1-rw* (red pericarp, white cob), and *p1-ww* (white pericarp, white cob) (Anderson 1924). To understand the mechanism underlying tissue-specific patterns, many of the *p1* alleles have been molecularly characterized and compared with one another (Chopra *et al.* 1998; Zhang and Peterson 2005a,b). For instance, molecular comparison of *P1-wr* and *P1-rr* revealed that *P1-rr* has a single-gene copy whereas *P1-wr* has a six-copy tandem-repeat structure (Chopra *et al.* 1998). Promoter swapping experiments indicated that the distinct expression patterns of *P1-wr* and *P1-rr* were not due to differences in their coding and proximal promoter sequences (Cocciolone *et al.* 2001). Rather, the DNA hypermethylation of *P1-wr* relative to *P1-rr* was associated with the absence of pericarp pigmentation (Chopra *et al.* 1998). In fact, the reduction of DNA methylation at *P1-wr* in the presence of an unlinked dominant modifier called *Unstable factor for orange1* (*Ufo1*) results in a corresponding range of pericarp (Chopra *et al.* 2003) and cob glumes (Sekhon *et al.* 2007) pigmentation. The tandem-repeat structure of the *P1-wr* allele is also present in many other naturally occurring maize germplasms, some of which have pericarp pigmentation, albeit it is restricted to the kernel gown (Brink and Styles 1966; Cocciolone *et al.* 2001). In these instances, DNA hypomethylation is correlated with the increased gene expression (Cocciolone *et al.* 2001). DNA hypermethylation has also been correlated with the suppressed state of a *P1-rr* epiallele called *P1-pr* (*p*atterned pericarp and *r*ed cob) (Das and Messing 1994). In this case, a DNAse I sensitivity assay demonstrated that the DNA hypermethylation of *P1-pr* correlates with chromatin condensation (Lund *et al.* 1995).

To identify putative cob- and pericarp-specific elements, the single-copy *P1-rr* allele has been extensively mutagenized using the *Ac* transposons, which resulted in a series of alleles showing a wide range of variegated pericarp and cob pigmentation (Athma *et al.* 1992).

Herein, we report the results based on 13 unique germinal *Mu*-insertion sites in the six-copy tandemly repeated *P1-wr* allele. Since *P1-wr* is multicopy, we knew that a mutation in any one copy (if all copies express) may not yield a phenotype. However, we also envisaged that the insertion of a *Mu* transposon might disrupt the epigenetic regulation of *P1-wr* gene expression (Barkan and Martienssen 1991; Girard and Freeling 2000; Cui *et al.* 2003). We recovered a single gain-of-pericarp-function allele, *P1-wr-mum6*, generated by a *Mu1* insertion in the 5′-UTR (of one of the copies in the P1-wr array). Interestingly, *P1-wr-mum6* expression is associated with the hypomethylation of a floral organ-specific enhancer sequence that is located at the 5′ end of every *P1-wr* gene copy. The position of this enhancer in the interrupted copy is distal from the *Mu1* insertion site and may lie near an adjacent upstream copy in the *P1-wr* tandem gene array. We discuss a mechanism through which the *Mu1* insertion in a single copy of *P1-wr* could lead to the increased expression.

MATERIALS AND METHODS

Maize stocks: The *P1-wr* [A632] inbred line was obtained from the Germplasm Resources Information Network (U.S. Department of Agriculture, Ames, IA). *p1-ww* [4co63] was obtained from the National Seed Storage Laboratory (Fort Collins, CO) while *P1-wr* [W23] was acquired from the Maize Genetics Cooperation Stock Center (Urbana, IL). *P1-rr-4B2* was obtained from Thomas Peterson (Grotewold *et al.* 1991a). The *P1-rr-4B2* allele was introgressed into the W23 background by six generations of backcrossing. A *Mu*-active stock was obtained from the Maize Genetics Cooperation (University of Illinois, Urbana–Champaign, IL). A stock carrying the dominant *Mu inhibitor* and the *Mu*-suppressible *Les28* reporter allele was kindly provided by Robert Martienssen, Cold Spring Harbor Laboratory (Cold Spring Harbor, NY) (Martienssen and Baron 1994). A stock heterozygous for *Mu killer* (*Muk*) was generously provided by Damon Lisch, University of California (Berkeley, CA) (Slotkin *et al.* 2003).

Identification of *Mu*-insertion lines in *P1-wr*: We used the Trait Utility System for Corn (TUSC) developed by Pioneer Hi-Bred International (Meeley and Briggs 1995) for transposon-based reverse genetics of *P1-wr*. In this procedure, *P1-wr* plants from several maize inbred lines were crossed with *Mu*-active plants that also carry a *P1-wr* allele and the resulting progeny plants were screened for *Mu* insertions. The *Mu*-active plants contain the autonomous *MuDR* transposase that induces the excision and transposition of itself as well as other, nonautonomous *Mu* elements (*Mu1–Mu12*). To identify *Mu* insertions, pooled DNA of a large population of the progeny plants was screened by PCR using *p1*-specific primers together with the *Mu*-*t*erminal *i*nverted *r*epeat (*Mu*-TIR) primer that is conserved in the border sequences of all *Mu* elements. Sequences of primers and their locations in *P1-wr* or *Mu1* are listed in supplemental Table 1. Positive pools showing PCR amplification were identified and products were subcloned into the pGemT-easy TA cloning vector (Promega, Madison, WI). Subsequently, the clones were sequenced to determine the positions of *Mu* insertions within the *P1-wr* gene. The *Mu*-element orientation of most insertion alleles could be discerned on the basis of unique SNPs in the TIRs (Dietrich *et al.* 2002; R. Meeley, unpublished data).

Genetic crosses with *P1-wr-mum6*: The *P1-wr-mum6* insertion line was identified in the F_1 of TUSC materials generated from a cross between the A632 inbred line and a stock carrying high *Mu* activity (see above). The F_2 progeny carrying the *P1-*

wr-mum6 insertion was screened for pericarp and cob pigmentation phenotypes. The F_2 plants were pollinated with *p1-ww* [4co63] and the resulting plants were reciprocally testcrossed with *p1-ww* [4co63]. To obtain *P1-wr-mum6* plants with inactive *Mu* elements, *P1-wr-mum6/p1-ww* [4co63] plants were crossed with a stock carrying the dominant *Mu inhibitor* and the *Mu*-suppressible *Les28* allele (Martienssen and Baron 1994). However, it has been shown that crosses with the *Mu inhibitor* stock do not always dominantly inactivate *Mu* activity (May *et al.* 2003). Thus, the *Mu* activity was followed in F_1 plants using the *Les28* reporter that confers a lesion-mimic phenotype only when *Mu* is active. Younger leaves sometimes appeared spotted, indicating that they retained *Mu* activity, whereas older leaves did not have spots, indicating that *Mu* had been inactivated. The F_2, F_3, and F_4 progenies also did not express the *Les28* phenotype and were thus considered to be *Mu* inactive. In some families the *Mu inhibitor* stock did not completely silence *Mu* activity (M. Robbins and S. Chopra, unpublished data). Thus, crosses were also made using the heterozygous *Mu killer* (*Muk*) stock, which was not available when this research was started. *Muk* is a naturally occurring partially deleted version of *MuDR* that contains an inverted repeat. *Muk* functions dominantly and is believed to facilitate RNA-dependent chromatin remodeling and silencing of functional *MuDR* elements (Slotkin *et al.* 2005). The presence of *Muk* in plants carrying *P1-wr-mum6* or *P1-wr* [A632] was determined using an established PCR-genotyping assay available at http://plantbio.berkeley.edu/~mukiller/using.html (Slotkin *et al.* 2003).

DNA gel blot analysis: Leaf genomic DNA was isolated using a modified CTAB method (Saghai-Maroof *et al.* 1984). DNA was digested to completion using enzymes, reagents, and incubation conditions from Promega. Digested DNA was fractionated on agarose gels and transferred to Nylon membranes, and the membranes were subsequently probed with DNA probes of interest. The DNA probes were labeled with [α-^{32}P]dCTP through random priming, using a Prime-It RmT random primer labeling kit (Stratagene, La Jolla, CA). Membranes were prehybridized for 4 hr at 65° in buffer containing NaCl (1 m), SDS (1%), Tris-HCl (10 mm), and salmon sperm DNA (0.25 mg/ml) followed by hybridization in the same buffer containing ^{32}P-labeled DNA probes for 16 hr at 65° (Athma and Peterson 1991). Membranes were washed twice in 0.1× SSC and 0.5% SDS at 65° for 15–30 min and exposed to X-OMAT film (Kodak, Rochester, NY). Blots were stripped of previous signal in boiling 0.1% SDS before they were reused.

RNA expression analysis: Pericarps and cob glumes were harvested 18 days after pollination and RNA was isolated using a modified phenol–chloroform extraction protocol (Verwoerd *et al.* 1989). RNA gel blot analysis was performed using 10 μg of total RNA from pericarp as previously described (Chopra *et al.* 1996). For RT–PCR analysis, 50 μg of total RNA was treated with DNase I (GIBCO-BRL, Gaithersburg, MD). Ten micrograms of treated RNA and 0.5 μg oligo $(dT)_{15}$ primer were denatured for 5 min at 70° and subsequently added to a reaction mixture containing ImProm-II reverse transcriptase (Promega). First-strand cDNA was synthesized by incubating the reaction mixture at 42° for 1 hr. The reverse transcriptase was deactivated by heating at 70° for 15 min. PCR primers of *P1-wr* that were used to amplify the first-stand cDNA templates are EP5-8 and SC2-2R (supplemental Table 1). EP5-8 is a forward primer that resides upstream of the *Mu1* insertion in *P1-wr-mum6* and was used with a reverse primer, SC2-2R, located downstream of the *Mu1* insertion (Figure 1). The large size of *P1-wr* intron 2 does not permit genomic DNA amplification between EP5-8 and SC2-2R. The housekeeping gene α-*tubulin* was used as an RT–PCR control.

Description of probe fragments: The region flanking the *Mu1* insertion in *P1-wr-mum6* was assayed with intron 2 probe fragments 8B and 8C, and the distal enhancer was assayed with probe fragment 15 (Lechelt *et al.* 1989; Chopra *et al.* 1998; Sekhon *et al.* 2007). *Mu* activity was assayed using gel blots made from *Hin*fI-digested genomic DNA (Chandler and Walbot 1986) and *Mu1* probe fragment was obtained by the amplification of pucMuED4 plasmid using M13 forward and reverse primers. The pucMuED4 plasmid was generously provided to by David Braun, Pennsylvania State University. Probes corresponding to *chalcone synthase* (*c2*) and *P1-rr* cDNAs have previously been described (Paz-Ares *et al.* 1986; Grotewold *et al.* 1991a).

Genomic bisulfite sequencing: Seedling leaf genomic DNA was extracted using a modified CTAB method (Saghai-Maroof *et al.* 1984). Eight micrograms of genomic DNA were restricted with suitable restriction enzymes to obtain ~1-kb fragments containing the region of interest. The restricted DNA was purified with phenol–chloroform and treated with sodium bisulfite, using a previously standardized protocol (Jacobsen *et al.* 2000; Sekhon *et al.* 2007). The upper strand of a 387-bp region from the distal enhancer (positions −5052 to −4666 of EF165349) was amplified using PCR primers specially designed to amplify DNA modified with sodium bisulfite (supplemental Table 1). Gel-purified PCR products were cloned using a TOPO TA cloning kit (Invitrogen, Carlsbad, CA) and sequenced using vector primers. Two plants each from the gain-of-function (*i.e.*, showing pericarp pigmentation) and nonexpressing (*i.e.*, with colorless pericarp) *P1-wr-mum6* families were analyzed and at least 20 clones per plant were sequenced.

RESULTS

Isolation of 13 heritable *Mu*-insertion sites in *P1-wr*: The TUSC germplasm was screened for *Mu* insertion in *P1-wr* using *Mu*-TIR and gene-specific primers (Figure 1). This region includes the proximal promoter and the downstream gene sequence containing exons 1 and 2, intron 1, and the 5′ end of intron 2. Thirteen heritable *Mu*-insertion sites were identified and these are listed 5′–3′ as *P1-wr-mum1–P1-wr-mum-13* in Table 1. Of these, 10 insertion alleles were commonly identified with two or more independent primer combinations. Three of the insertion sites were associated with multiple independent *Mu* insertions. For example, *P1-wr-mum9* (position 471) and *P1-wr-mum12* (position 702) were selected twice while *P1-wr-mum13* (position 760) was selected three times. Four *Mu* insertions were in the promoter region and three were found each in exons 1 and 2. Two insertion sites were identified in intron 1 and a single site was found in the beginning of intron 2. The types of *Mu* elements found in *P1-wr* were *Mu1*, *Mu4*, *Mu8*, *Mu11*, and *MuDR* (Table 1). Additionally, one *Mu* insertion had a TIR that resembled the published sequence of *Mu1*, but it contained SNPs at two positions (Barker *et al.* 1984). Since the region internal to the TIR was not sequenced, it is currently denoted as a *Mu1*-like element.

***P1-wr-mum6* is associated with gain of function in pericarp tissue:** F_2 progeny plants of all 13 *P1-wr*-specific *Mu*-insertion events were analyzed for altered pigmentation patterns. Loss-of-function phenotypes, such as

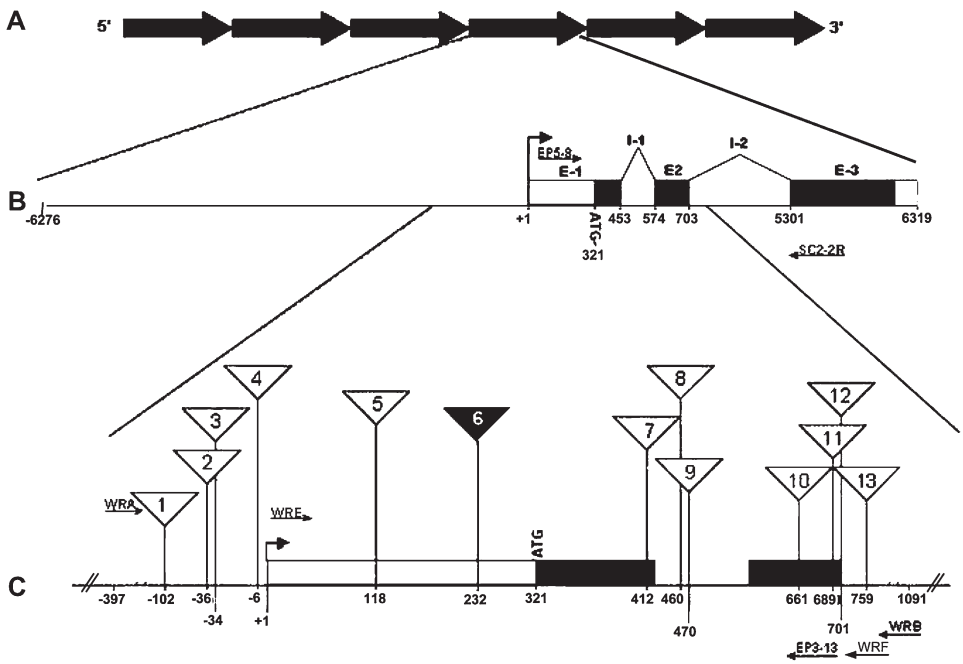

D

Primer Combination	Template used	Experiment	Product Size	*P1-wr* Copy (s) amplified
WRA +*Mu*-TIR	Genomic DNA	Genotyping	713 bp	*Mu1* containing copy
Mu-TIR + WRB	Genomic DNA	Genotyping	941 bp	*Mu1* containing copy
Mu-TIR + EP3-13	Genomic DNA	Genotyping	442 bp	*Mu1* containing copy
EP5-8 + EP3-13	Genomic DNA	Genotyping	500 bp	Wild type copy(s)
WRE + WRF	Genomic DNA	Genotyping	801 bp	Wild type copy(s)
EP5-8 + SC2-2R	cDNA	Gene Expression	498 bp	Wild type copy(s)

FIGURE 1.—*Mutator* element insertion sites in *P1-wr*. (A) Illustration depicting the tandem repeats that make up the six-copy *P1-wr* complex. (B) Gene structure of one representative *P1-wr* copy in which exons (E) and introns (I) are shown. A bent arrow indicates the position of the transcription start site that is represented as +1. Positions of primers that were used for expression analysis of *P1-wr-mum6* (see below) are represented by arrows. (C) Enlarged region of exon 1, intron 1, and the 5′ end of intron 2 showing the position of *Mutator* transposon insertions (triangles). Numbers inside the triangles correspond to the insertion lines (*P1-wr-mum1*–*P1-wr-mum13*) presented in Table 1. The solid triangle designates the gain-of-function mutation *P1-wr-mum6*. Primers that were used with genomic DNA to characterize the insertion lines are indicated as arrows. (D) Details of the PCR-based characterization of the *P1-wr-mum6* allele. The amplification product size and the type of *P1-wr* copy amplified are listed for each experiment described in the text. *P1-wr* primers positioned 5′ and 3′ to the *Mu1* insertion were used to amplify cDNA to determine the gene expression originating from wild-type copy (or copies).

the reduction in cob pigmentation, were not observed in any insertion line. Interestingly, one insertion line, *P1-wr-mum6*, exhibited a gain-of-pericarp-pigmentation phenotype. PCR amplification and sequence characterization of the *P1-wr-mum6* insertion allele revealed that a *Mu1* element is located in direct orientation in the 5′-UTR, 232 bp 3′ to the transcription start site of *P1-wr* (Figure 1; Table 1). DNA gel blot analysis was also performed to compare the structure of *P1-wr* with *P1-wr-mum6* (Figure 2). Genomic DNA of these genotypes was digested with *Nco*I (Figure 2A). The *p1* fragment 8B was used as a probe because it resides downstream of the *Mu1* insertion site in *P1-wr-mum6*. In *P1-wr*, *Nco*I digestion produces a 5.5-kb fragment. Conversely, in *P1-wr-mum6*, *Nco*I cuts in both *P1-wr* and *Mu1*, yielding a 4.2-kb fragment (see Figure 2B). The weak hybridization signal of the *P1-wr-mum6*-specific band (4.2 kb) relative to the *P1-wr*-specific band (5.5 kb) strongly suggests that the *Mu1* insertion is in one of the copies of *P1-wr*.

The gain-of-function allele *P1-wr-mum6* was initially discovered as red stripes on colorless pericarp of ~1 in every 10 F_2 kernels (see kernel marked "P" in the section labeled "S" in Figure 3A). However, the pericarp pigmentation phenotype was present in only a single ear of a total of 15 ears recovered from the F_2 plants (see Figure 3A, sections 1 and 2). Genotyping of nine individuals that had colorless pericarp revealed that eight carried the *P1-wr-mum6* allele (see Figure 3A, section 2). The single gain-of-function *P1-wr-mum6* ear had four kernels that displayed red sectored pericarp pigmentation (Figure 3A, section 1). In summary, the gain of pericarp phenotype of *P1-wr-mum6* in early generations was associated with low expressivity and poor penetrance.

Gain-of-pericarp-function as well as colorless-pericarp kernels carrying the *P1-wr-mum6* allele were further followed to perform genetic and molecular tests. Reciprocal *P1-wr-mum6/p1-ww* [4co63] × *p1-ww* [4co63] testcross progenies were characterized from a single dark uniform kernel, two sectored kernels, and four colorless kernels. This was done to determine if there was a correlation between the pigmentation of the testcross progenies (Figure 3B, sections a–c) and that of their progenitor kernels (Figure 3A, section 1). Interestingly, the level of pericarp pigmentation in each testcross progeny (Figure 3B, sections a–c) did correspond with the level of pigmentation present on the parental *P1-wr-mum6/p1-ww* kernel (Figure 3A, section

TABLE 1

Positions of *Mu* insertions in *P1-wr*

Insertion line	Distance from TSS[a]	*P1-wr* region	*Mu* element(s) types, orientation[b]	Target sequence[c]
P1-wr-mum1	−102	Promoter	*Mu1*, R	AATTCGG**TCGGTCCGT**AACGTGC
P1-wr-mum2	−36	Promoter	*Mu1*, F	CGTCCGC**TGCTATATT**ATGGCCG
P1-wr-mum3	−34	Promoter	*Mu11*, F	TCCGCTG**CTATATTAT**GGCCGGC
P1-wr-mum4	−6	Promoter	*MuDR*, ND	CGTGCCC**TCTCTAGCC**AGCACAG
P1-wr-mum5	+118	Exon 1	*Mu4*, ND	CACCAAC**TCCCTTGGA**CGCACGC
P1-wr-mum6	+232	Exon 1	*Mu1*, R	TCCGGTG**TGGCCAGCG**GCGGCCG
P1-wr-mum7	+412	Exon 1	*Mu1*, F	TGCGGA**GCACGGCGA**GGGGTCC
P1-wr-mum8	+460	Intron 1	*MuDR*, ND	TAAACC**AAAGCCGGC**CGCGCGC
P1-wr-mum9	+470	Intron 1	*Mu1*, F; *Mu1*, F	GCCGGCC**GCGCGCCAT**GCATCGC
P1-wr-mum10	+661	Exon 2	*Mu1*, R	AGGAGGA**AGAAGACAT**CATCATC
P1-wr-mum11	+689	Exon 2	*Mu1*, F	CCACGCC**ACCCTCGGC**AACAGGT
P1-wr-mum12	+701	Exon 2	*Mu1*, R; Mu8, F	CGGCAAC**AGGTAACAA**TAAGCGC
P1-wr-mum13	+759	Inron 2	*MuDR*, ND; *Mu1*, F; *Mu1*-like[d], ND	TAGAGAG**TAGTAGTAC**TACTACT

[a] TSS, transcription start site. The positions of insertions correspond to *P1-wr* sequence accession EF165349.
[b] F, forward orientation; R, reverse orientation; ND, orientation not determinable.
[c] The predicted 9-bp target sites of the *Mu* insertions are indicated in boldface type. Accession no. of *P1*-wr: EF165349.
[d] *Mu1*-like denotes presence of two SNPs in the TIR sequence that resembles *Mu1* (accession no. X00913). SNP positions are underlined in the TIR sequence: 5′-GAATCCCCTTCCCTCTTCGTCCACAATGGCAGTTATC-3′.

1). However, the level of pericarp pigmentation did not depend on which parent (*P1-wr-mum6* or *p1-ww* [4co63]) was used as the pollen source. The testcross progeny developed from the colorless kernels remained colorless, indicating that the suppressed state of *P1-wr-mum6* had become stable (Figure 3B, section a). The sectored kernels gave rise to progeny ears either with colorless pericarp (~70%) or with occasional red pericarp stripes (~30%) (Figure 3A, section b). Therefore, the penetrance and expressivity of the pericarp-pigmentation phenotype associated with the progeny of the sectored kernels remained low. The fully red kernel generated a stable testcross progeny in which all *P1-wr-mum6* individuals had a range of red pericarp pigmentation (Figure 3B, sections c and d). PCR genotyping of pericarp DNA from *P1-wr-mum6/p1-ww* testcross progenies "a" and "c" confirmed that the *Mu1* insertion was present even though pericarp pigmentation was not observed (Figure 3C).

The progeny ears resulting from the dark red kernel (testcross progeny c) had the expected 1:1 ratio of red to colorless pericarp (see Table 2). This showed that the gain-of-pericarp-pigmentation phenotype was stably inherited. However, sibling plants from this population differed with respect to the level of pericarp pigmentation (Figure 3B, section d). The pericarp pigmentation was either uniformly diffused or localized to the silk attachment point or kernel gown. In addition, a small number (~5%) of ears displayed a kernel-to-kernel variation in overall pigment accumulation. Since all pigmented individuals were heterozygous, the range in pericarp pigmentation could not be due to a dosage effect.

To ensure that the gain of function in *P1-wr-mum6* was not due to an unlinked mutation, we crossed a *P1-wr-mum6/p1-ww* [4co63] individual with *P1-wr* [W23]. The resulting F_1 plant was crossed with *p1-ww* [4co63] to segregate *P1-wr-mum6* from *P1-wr* [W23]. If the gain of function was due to unlinked mutations, we would expect pigmented pericarp in *P1-wr* [W23]/*p1-ww* [4co63] individuals. This cross yielded a 1:1 ratio of red to colorless pericarp, indicating that the *P1-wr-mum6* stock did not contain a secondary mutation that can induce expression of naive *P1-wr* in pericarp (Table 2). Moreover, this result indicated that the *P1-wr-mum6* allele does not interact in *trans* with *P1-wr* [W23].

The expression of linked uninterrupted gene copy (or copies) is elevated in *P1-wr-mum6*: To test if the gain of pigmentation in *P1-wr-mum6* was due to the increased expression of *p1* and a *p1*-regulated structural gene, *chalcone synthase* (*c2*), we performed RNA gel blot analysis (Grotewold *et al.* 1991b, 1994). The C2 protein catalyzes the first committed enzymatic step in the production of phenylpropanoid compounds including flavonoid pigments (Kreuzaler and Hahlbrock 1975). As expected, when compared with *P1-wr, P1-wr-mum6* had a large increase in *p1* and *c2* steady-state transcripts in pericarp tissue (Figure 4A). Interestingly, *P1-wr-mum6* and the single-copy *P1-rr-4B2* allele were expressed at nearly the same level.

The increased expression in *P1-wr-mum6* could arise from two sources: new transcripts may originate from the gene copy containing the *Mu1* insertion in the 5′-UTR, or there may be increased expression from one or more of the five other (wild-type) copies that are not interrupted by the transposon insertion. Elevated expression of the interrupted copy could be explained if the *Mu1* element in the 5′-UTR functions as a cryptic promoter for the immediate downstream gene copy. For example, the suppression of the maize *hcf106* mutation

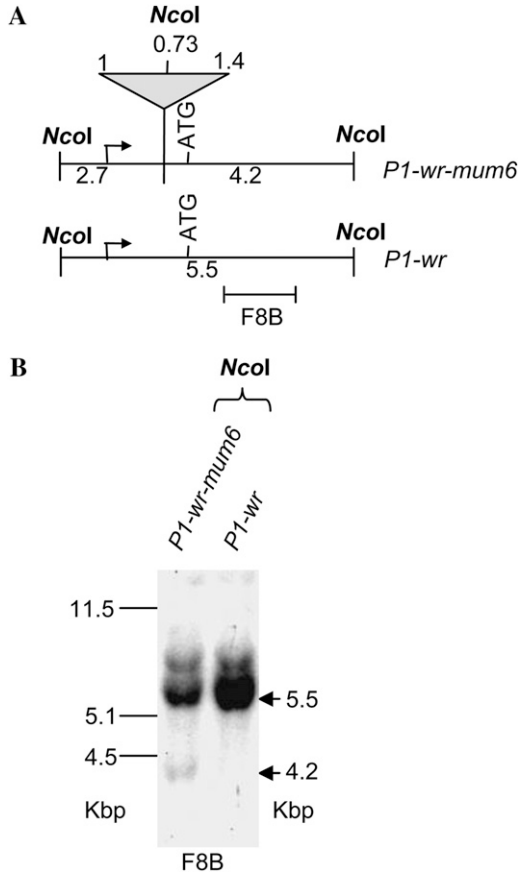

FIGURE 2.—Structural comparison of *P1-wr-mum6* and *P1-wr* [A632] alleles. (A) Restriction map showing the positions of *Nco*I sites in *P1-wr-mum6*. The triangle signifies the *Mu1* insertion in *P1-wr-mum6*. Fragment sizes are indicated for both the transposon-interrupted (*P1-wr-mum6*) and wild-type (*P1-wr*) copies. (B) DNA gel blot analysis of *P1-wr-mum6* showing the presence of a *Mu1* insertion. The location of *p1* probe fragment 8B is shown below the restriction map in A. Arrows indicate the position of expected sizes (in kilobase pairs) of specific bands, after *Nco*I digestion. Sizes of the molecular weight marker bands in kilobase pairs are shown on the left of the blot.

has been directly related to the presence of *hcf106* transcripts that originate downstream of a *Mu1* element (BARKAN and MARTIENSSEN 1991). Several experiments were conducted to detect transcripts that may be arising from the *P1-wr* copy containing the *Mu1* insertion. RT–PCR analysis using the *Mu*-TIR and EP3-13 primers did not detect any transcript originating within the *Mu1* element (data not shown). Additionally, primer extension and 5′ rapid amplification of cDNA ends (RACE) PCR experiments performed using *P1-wr-mum6* and *P1-wr* control plants also failed to detect different transcript initiation sites. All detected transcripts contained the transcription start site expected for wild-type *P1-wr* (data not shown). Moreover, RNA gel blots also did not reveal the presence of any aberrantly sized transcripts (Figure 4A). These results suggested that the interrupted copy is nonfunctional and that the increased expression in *P1-wr-mum6* may originate from one or more of the uninterrupted copies.

To confirm that the enhanced RNA expression of *P1-wr* originates from wild-type copies, RT–PCR analysis was performed (Figure 4B). We used a primer EP5-8, which resides upstream of the *Mu1* insertion in *P1-wr-mum6*, and SC2-2R, which is located downstream of the *Mu1* insertion (see Figure 1B for position of primers). The presence of the *Mu1* element would prohibit amplification of transcripts containing the insertion. This assay specifically yielded products with the size expected from uninterrupted *P1-wr* copy (or copies). Importantly, the range in pericarp pigmentation was directly proportional to the abundance of the *p1* transcripts detected through RT–PCR (Figure 4B). However, the pigmentation and *p1* gene expression were similar in *P1-wr* and *P1-wr-mum6* cob glumes (Figure 4B). This suggests that the upregulation in pericarp in *P1-wr-mum6* is achieved through a tissue-preferred mechanism. It is conceivable that the *Mu1* insertion disrupted a suppression mechanism that is normally operative in *P1-wr* pericarp tissue. In summary, these results support the hypothesis that the uninterrupted copies are the source of the *p1* expression in *P1-wr-mum6* pericarps.

***P1-wr-mum6* DNA hypomethylation correlates with pericarp pigmentation:** DNA gel blot data indicated that *P1-wr-mum6* contains a six-copy structure similar to that of *P1-wr*, except that a single copy is interrupted by *Mu1* (Figure 2 and our unpublished results). It is known that transposon insertions in genes or in their neighboring regions can affect expression and epigenetic states of such genes (LIPPMAN *et al.* 2004). We therefore hypothesized that the *Mu1* insertion in *P1-wr-mum6* may have induced epigenetic changes of the multicopy complex, thereby altering its expression. To test if DNA methylation changes correlate with pericarp pigmentation in *P1-wr-mum6*, seedling leaf DNA was digested with the methylation-sensitive restriction enzyme *Hpa*II and gel blots were hybridized with *p1* probe fragment 15. The banding pattern of several genotypes was compared. First, the *P1-wr* sources that were used to generate *P1-wr-mum6* were compared with *P1-wr-mum6* and *P1-wr* F_2 individuals of the TUSC screen that had colorless pericarp. These genotypes yielded similar ~12.0-, 7.9-, and 0.4-kb bands, indicating that the DNA methylation was unaltered in *P1-wr-mum6* plants that have colorless pericarp (Figure 5A). Second, to address whether DNA methylation changes are associated with pericarp pigmentation in *P1-wr-mum6*, the different *p1-ww* × *P1-wr-mum6/p1-ww* testcross progenies (see Figure 3) were also analyzed. The *P1-wr-mum6* progeny that exhibited colorless pericarp (Figure 3B, section a) or possible occasional red stripes (Figure 3B, section b) had no detectable DNA methylation differences when compared with *P1-wr* (Figure 5; see lanes marked a or b). Only in the fully penetrant progeny with relatively high levels of pericarp pigmentation (Figure 3B, sections c and d, and Table 2)

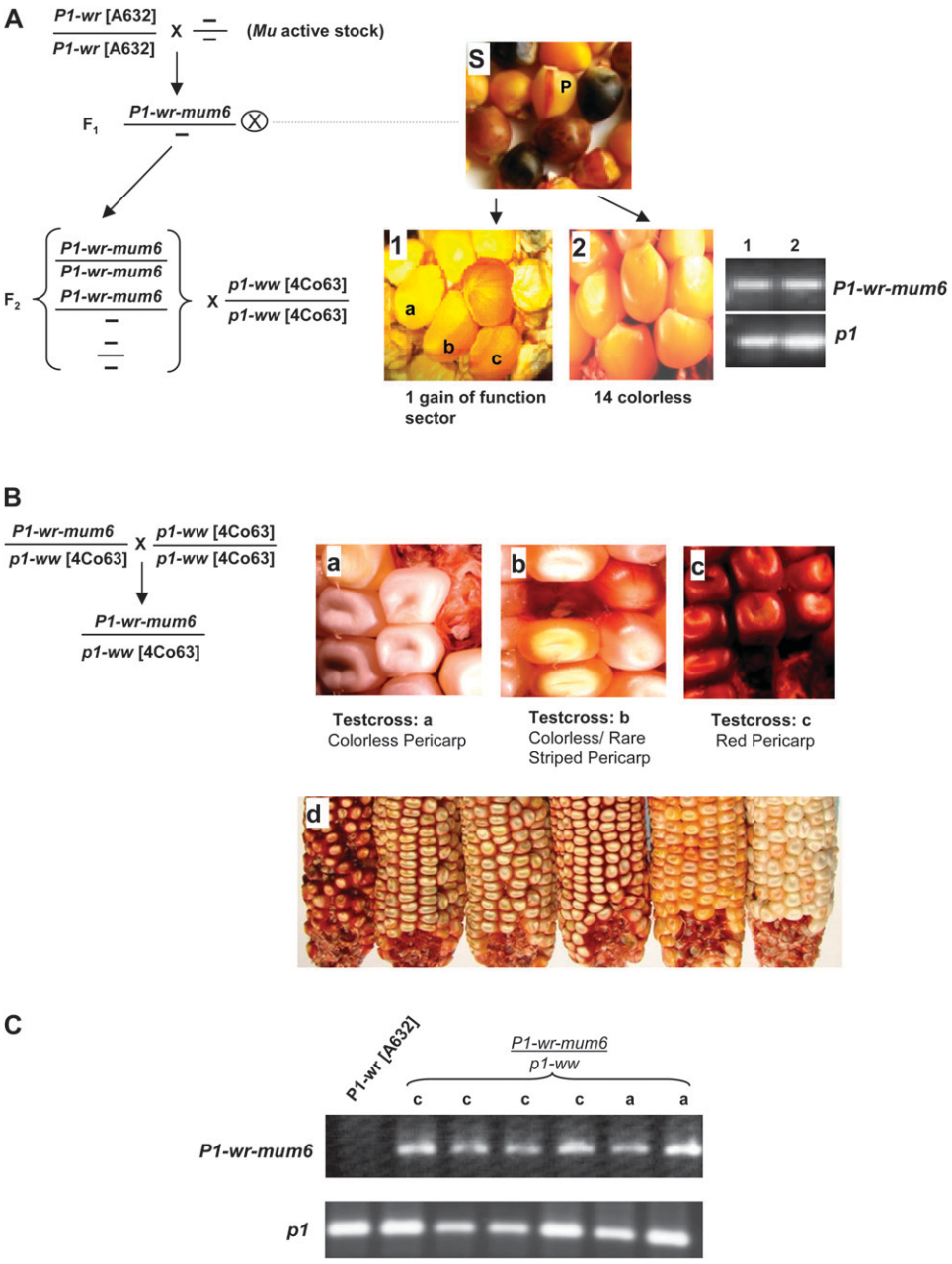

FIGURE 3.—Progression of pericarp pigmentation in *P1-wr-mum6*. (A) The gain of pericarp pigmentation associated with *P1-wr-mum6* initially had low expressivity and penetrance. The F_2 source seed of *P1-wr-mum6* had red phlobaphene stripes (section S, see kernel marked "p"). F_2 plants grown from seeds shown in section S were crossed with *p1-ww* [4co63]. Phenotypes of two representative crossed ears are shown in sections 1 and 2. All F_2 plants were genotyped by PCR for the presence of *P1-wr-mum6*, using the *Mu*-TIR and WRB primers (see Figure 1D). The *p1* primers WRE and WRF were used to amplify regions of the *P1-wr* gene copies that do not contain the transposon insertion. Representative lanes of PCR-amplification products of individuals in sections 1 and 2 are shown on the right. A kernel map was constructed from the F_3 ear in section 1 by lettering the kernel types a–c. (B) Plants grown from kernels marked a–c in section 1 of A were reciprocally crossed with *p1-ww* [4co63]. Pericarp phenotypes of representative testcross progeny ears are shown in sections a–c. Section d shows the variability in ear phenotypes that is apparent in testcross progeny c. (C) Presence of *P1-wr-mum6* in the testcross progenies a and c was determined by PCR amplification of pericarp DNA using the *Mu*-TIR and EP3-13 primers (see Figure 1D). The *p1* primers EP5-8 and EP3-13 were used to amplify regions of the uninterrupted *P1-wr* copies. Lanes marked a and c designate *P1-wr-mum6/p1-ww* [4co63] individuals obtained from test crosses a and c (see ears a and c in B), respectively.

did we detect DNA hypomethylation (Figure 5, see lanes marked c). The hypomethylation consisted of three *Hpa*II bands of ~5.1-kb, 2.9-kb, and 500-bp sizes. However, these DNA methylation changes were not detected using intron 2 probe fragments 8B and 8C, indicating that the affected *Hpa*II sites may reside in the upstream promoter region encompassing fragment 15 (Figure 5B). In fact, the 500-bp fragment has been previously reported to arise from hypomethylation of *Hpa*II sites in an upstream promoter region (CHOPRA *et al.* 2003). Interestingly, this region has been shown to be part of a distal enhancer (Figure 5B) for *p1* expression in pericarp tissue (SIDORENKO *et al.* 2000; CHOPRA *et al.* 2003).

The aforementioned DNA gel blot results indicated that the distal enhancer region may be hypomethylated in *P1-wr-mum6* plants that have ectopic gain-of-pericarp pigmentation. This result, although promising, reported hypomethylation of only a single *Hpa*II site within the distal enhancer region. It therefore was hypothetically possible that the hypomethylation of this site did not reflect the DNA methylation status of the broader distal enhancer region (Figure 5B). To determine the cytosine methylation across a region encompassing the 3′ end of the distal enhancer (*i.e.*, positions −5052 to −4666 of *P1-wr* accession EF165349), we used genomic bisulfite sequencing. For this analysis, we compared *P1-wr-mum6* expresser plants from the fully penetrant testcross family

TABLE 2

Analyses of testcross populations showing the linkage between the presence of the *P1-wr-mum6* allele and the gain of pericarp pigmentation

Genotype	Parental ear	Subset of 50 plants			Total	
		PCR+, PC+	PCR+, PC−	PCR−, PC−	PC+	PC−
p1-ww[4co63] × *P1-wr-mum6* *p1-ww*[4co63] (from progeny c in Figure 3)	PC+	23	0	27	36	35
P1-wr-mum6 × *p1-ww* [4co63] *P1-wr* [W23]	PC+	ND	ND	ND	40	42

PC+ and PC− denote the presence and the absence of pericarp pigmentation, respectively. PCR+ individuals (*P1-wr-mum6*) were identified on the basis of the presence of a 941-bp amplification product using the *Mu*-TIR and WRB primer pair. ND, PCR genotyping was not done.

c with nonexpresser plants from testcross family a that exhibited no gain-of-pericarp pigmentation (see Figure 3B, sections a and c). Interestingly, bisulfite sequencing results showed that the *P1-wr-mum6* expresser plants were hypomethylated at all CG sites and at all but one CNG sites (Figure 6, A and B). Therefore, nearly the entire distal enhancer region tested was hypomethylated in *P1-wr-mum6* expressers. The combined reduction in the assayed region was 30.3% for CG and 24.4% for CNG methylation (Figure 6C). CHH methylation levels were negligible at all sites regardless of *P1-wr-mum6* expression (Figure 6C and supplemental Figure 1).

***P1-wr-mum6* expression is not affected by *Mu* activity:** The DNA hypomethylation at the *p1* distal enhancer may be induced by the presence of the *Mu1* insertion into the 5′-UTR by at least three mechanisms: (1) the MuDR transposase could affect *trans*-factors that regulate gene expression mechanisms, (2) the DNA methylation at the *Mu1* element could spread to the flanking *P1-wr* sequence, or (3) the transposon interruption itself could physically interfere with *cis*-regulatory regions that are important for local chromatin remodeling. We tested each of these possibilities and these are presented in the following text.

The activity of the MuDR transposase can interfere with gene expression mechanisms such as promoter function, intron splicing, and polyadenylation (Barkan and Martienssen 1991; Girard and Freeling 2000; Cui *et al.* 2003). To determine if such *Mu* suppression mechanisms were altered in *P1-wr-mum6* plants with ectopic pericarp pigmentation, we tested the *Mu* activity status of the aforementioned *p1-ww* × *P1-wr-mum6/p1-ww* testcross progenies that had distinct levels of pericarp pigmentation (see Figure 3B, sections a–c). We used a previously described *Mu* activity assay that relies on the fact that all inactive *Mu* elements in the genome (including *MuDR*) are coordinately methylated (Chandler and Walbot 1986; Lisch *et al.* 1995; Lisch 2002). Seedling leaf genomic DNA was digested with *Hin*fI and the resulting blot was hybridized with a *Mu1* probe. *Hin*fI sites are methylated when *Mu1* is in an inactive state, which is evidenced by the loss of a 1.3-kb band and the presence of several higher-molecular-weight fragments (Chandler and Walbot 1986; Lisch *et al.* 1995). All testcross progeny plants showed hypomethylated *Mu1* elements, indicated by the presence of the 1.3-kb band. Therefore, despite the differences in pericarp pigmentation in the testcross progenies, there was no difference in the DNA methylation of *Mu1* (Figure 7A).

The idea that the DNA methylation at *Mu* elements can affect the DNA methylation and expression of an adjacent gene sequence was established for a *Mu*-insertion allele of *hcf106* (Martienssen *et al.* 1990). In the case of the *knotted1* gene, the severity of the *Knotted1-mum7* mutant phenotype was directly correlated with the degree of *Mu1* hypomethylation (*i.e.*, *Mu* activity) (Greene *et al.* 1994). To test whether the presence of *Mu* activity positively affects pericarp pigmentation of *P1-wr-mum6*, we developed a *Mu* inactive *P1-wr-mum6* stock through crosses with a stock carrying *Mu inhibitor* (see materials and methods). Absence of a 1.3-kb *Hin*fI fragment and presence of higher molecular weight (*e.g.*, 2.8 kb) demonstrated *Mu* elements were silenced in these individuals (Figure 7B). Ear phenotypes revealed that the pericarp pigmentation was also present in the absence of *Mu* activity. Furthermore, *P1-wr-mum6* individuals from a testcross population that exhibited a range of pericarp pigmentation (see Figure 3B, section d) did not have a corresponding range of *Mu1* methylation (See Figure 7B, bottom). In summary, these results demonstrate that the activity of MuDR does not affect the *P1-wr-mum6* phenotype.

A similar genetic approach was undertaken when *Mu killer* (*Muk*) became available in the laboratory of Damon Lisch. Like *Mu inhibitor*, the presence of *Muk* dominantly silences *MuDR* expression albeit in a more consistent fashion (May *et al.* 2003; Slotkin *et al.* 2003, 2005). *P1-wr* and *P1-wr-mum6* plants differing for the presence of *Muk* were identified using a PCR assay

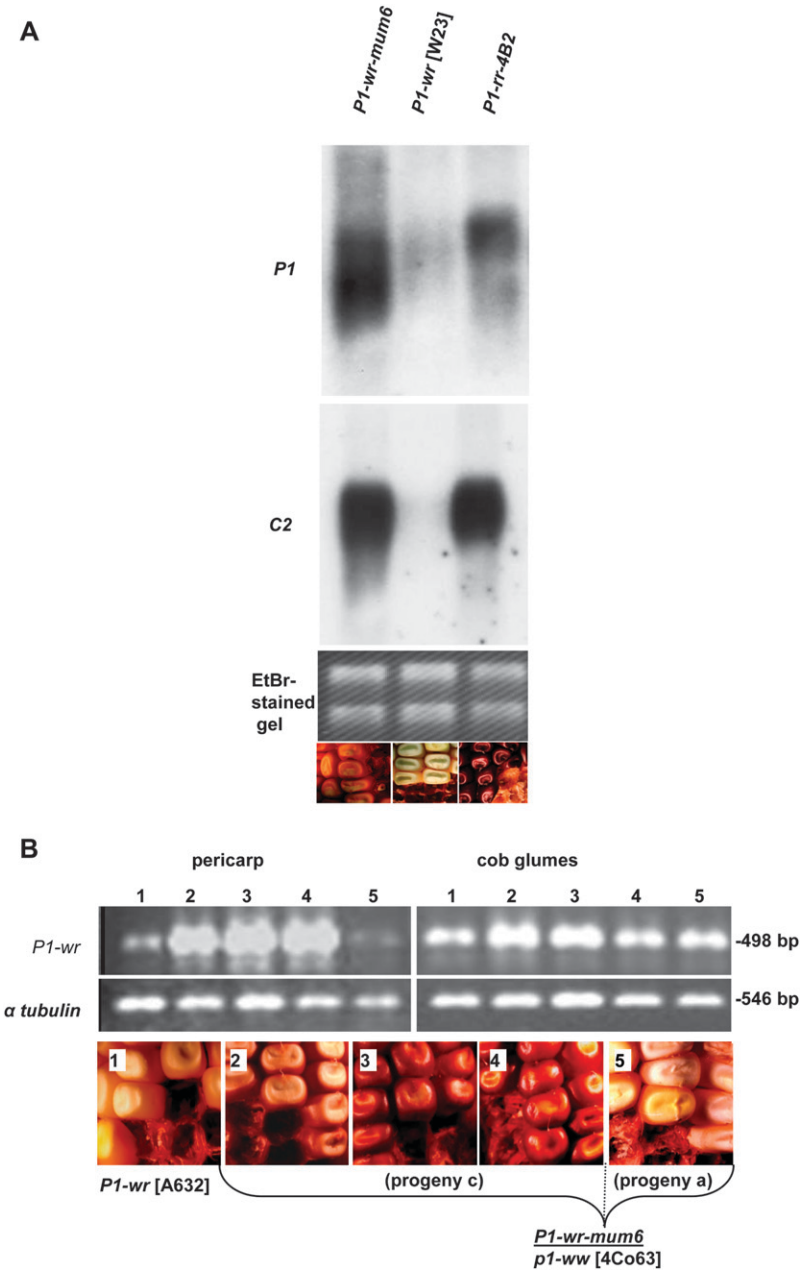

FIGURE 4.—Gain of pericarp pigmentation in *P1-wr-mum6* results from upregulation of *P1-wr*. (A) RNA gel blot showing increased steady-state transcript level of *p1* and *c2* in *P1-wr-mum6* as compared to *P1-wr*. The *P1-rr-4B2* pericarp RNA was used as a positive control. Phenotypes of the three alleles are shown below the gel picture. (B) Reverse-transcription–PCR was used to compare the *p1* expression in pericarp and cob glumes of *P1-wr-mum6/p1-ww* [4Co63] and homozygous *P1-wr* [A632] individuals. Primers EP5-8 and SC2-2R were used to amplify the first-strand cDNA (see Figure 1D). The amplified product of 498 bp results from the expression of the wild-type copy (or copies) of *P1-wr-mum6* that does not contain the *Mu1* insertion. Numbered lanes correspond with sections indicated below the gel picture. Section 1 is *P1-wr* [A632], and sections 2–4 show *P1-wr-mum6/p1-ww* [4co63] ears from the testcross progeny "c" (see Figure 3) that was derived from a fully red kernel. Section 5 shows a *P1-wr-mum6/p1-ww* [4co63] ear from the testcross progeny a (see Figure 3) that was derived from a colorless *P1-wr-mum6/p1-ww* [4co63] kernel.

(Figure 8A; MATERIALS AND METHODS). In the individuals carrying *Muk*, inactivity of *Mu* elements was confirmed by digesting leaf genomic DNA with *Hin*fI and hybridizing the blots with a *Mu1* probe (data not shown). As expected, the presence of *Muk* had no effect on the pericarp pigmentation in *P1-wr-mum6* (Figure 8A, bottom). To test if the *Mu* activity has any effect on the *P1-wr-mum6* epigenetic state, DNA methylation of different regions of *P1-wr-mum6* was assayed by gel blot analysis. We observed that the presence of *Muk* does not affect the DNA methylation status of *P1-wr-mum6* at *p1* intron 2 and distal enhancer regions (Figure 8B). In summary, the status of *Mu* activity does not seem to affect *P1-wr-mum6* expression and its DNA methylation status.

DISCUSSION

The numerous alleles of *p1* that differ with respect to gene structure and tissue specificity are valuable tools for studying how copy number may regulate tissue-specific expression patterns. However, the importance of *p1* gene copies in tissue-specific expression is not very well understood. Copy number does not have a clear role in governing *p1* expression patterns because several *p1* alleles that have similar multicopy gene structures to *P1-wr* have red pericarp; however, the pigmentation is not as uniform or intense as that of the single-copy *P1-rr* allele (COCCIOLONE *et al.* 2001). Additionally, the *P1-pr* epiallele of *P1-rr* has suppressed (patterned) pericarp pigmentation despite being single copy (DAS and

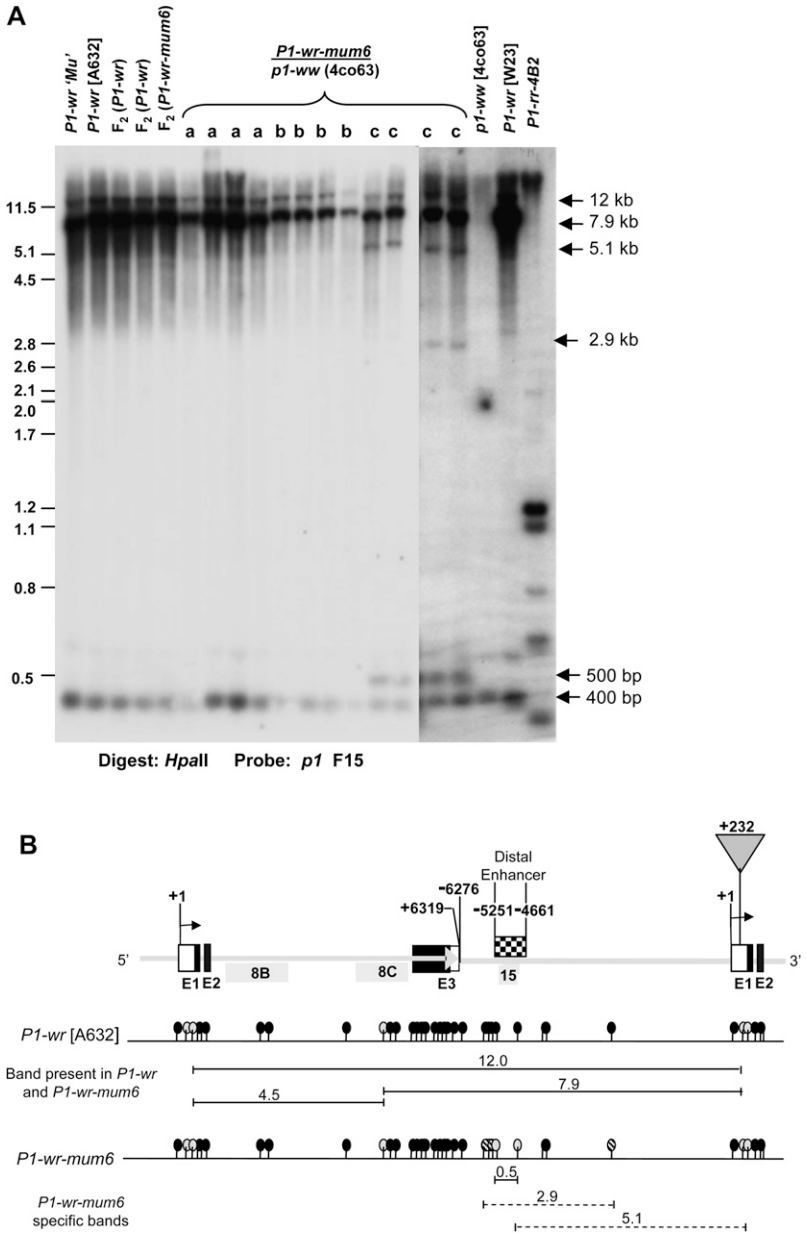

FIGURE 5.—Gain of pericarp function in *P1-wr-mum6* correlates with the hypomethylation of a distal enhancer sequence of *P1-wr.* (A) Seedling leaf DNA was digested with *Hpa*II and gel blots were hybridized with *p1* fragment 15 that corresponds to the distal enhancer element of the *p1* gene (LECHELT *et al.* 1989; SIDORENKO *et al.* 2000). Arrows on the right side of the blot denote the location of specific bands discussed in the text. Genotypes are shown on the top of the gel picture. These include the *P1-wr* parental sources used in the TUSC screen to generate *P1-wr-mum6,* F_2 generation *P1-wr* and *P1-wr-mum6* individuals that had colorless pericarp, and *P1-wr-mum6/p1-ww* [4co63] individuals derived from testcross progenies a–c (Figure 3). These testcross progenies are shown by the letters a, b, and c, respectively. The *Mu*-active source used to generate *P1-wr-mum6* is denoted by *P1-wr* '*Mu*'. (B) Gene structure diagram showing two representative partial copies of the six-copy tandem gene array. The coordinates shown above the diagram correspond with the *P1-wr* accession EF165349. The positions of exons 1–3 (E1–E3) are given as rectangles where the open regions of exons 1 and 3 correspond with the 5′- and 3′-UTRs, respectively. The location of the *Mu1* transposon in the 5′-UTR of *P1-wr-mum6* is represented as a shaded inverted triangle. However, it is important to note that it is not known at this point which *P1-wr* copy carries the insertion. The distal enhancer that is present in each gene copy is shown as a checkered box. The *p1* probe fragments used for construction of the methylation map are shown as shaded rectangles below the gene structure diagram. The DNA methylation status at *Hpa*II sites (ovals) is based on gel blot results shown in A and in Figure 8B. Solid ovals represent hypermethylated sites, shaded ovals are partially methylated sites, and hatched ovals indicate partially methylated sites. Band sizes are shown as horizontal lines below the *Hpa*II sites; dashed lines indicate estimated band locations because of close proximities of *Hpa*II sites

MESSING 1994). However, it is noteworthy that there has not been a report of functional single-copy *p1* alleles with colorless pericarp.

Similar to *Ac* transposon insertions in *P1-rr* (GROTEWOLD *et al.* 1991B), there are specific sites within the 5′ end of *P1-wr* that are candidates for *Mu*-insertion hotspots. The identified *Mu*-insertion clusters even contained instances in which distinct *Mu* elements incorporated at the same sequence context. Since *P1-wr* is a multiple-copy gene and several *P1-wr* inbred lines

FIGURE 6.—The correlation between DNA hypomethylation and pericarp pigmentation in *P1-wr-mum6* was examined by genomic bisulfite sequencing. Leaf genomic DNA of *P1-wr-mum6* expresser (*i.e.*, showing red pericarp pigmentation) and nonexpresser plants (*i.e.*, showing colorless pericarp) was used to study cytosine methylation of a distal enhancer (location shown in Figure 5B). We specifically assayed a 387-bp fragment that is located at the 3′ end of the distal enhancer (positions −5052 to −4666 of *P1-wr* accession EF165349). Methylation of individual CG and CNG sites in this region are shown in A and B, respectively. The position of the sites is shown on the *x*-axis while the percentage of methylation is presented on the *y*-axis. The percentage of methylation for each residue was calculated by dividing the methylated clones for that residue by the total number of clones. Two expresser and two nonexpresser plants were studied and the averages are presented here. CGG sites were counted as CG sites. (C) Cumulative methylation in CG, CNG, and CHH (H is A, C, or T) context in the genotypes studied. For each genotype, overall methylation in each context was calculated by dividing the number of methylated cytosines by the total number of cytosines in the context in all the clones. Context of methylation is shown on the *x*-axis and percentage of methylation is shown on the *y*-axis.

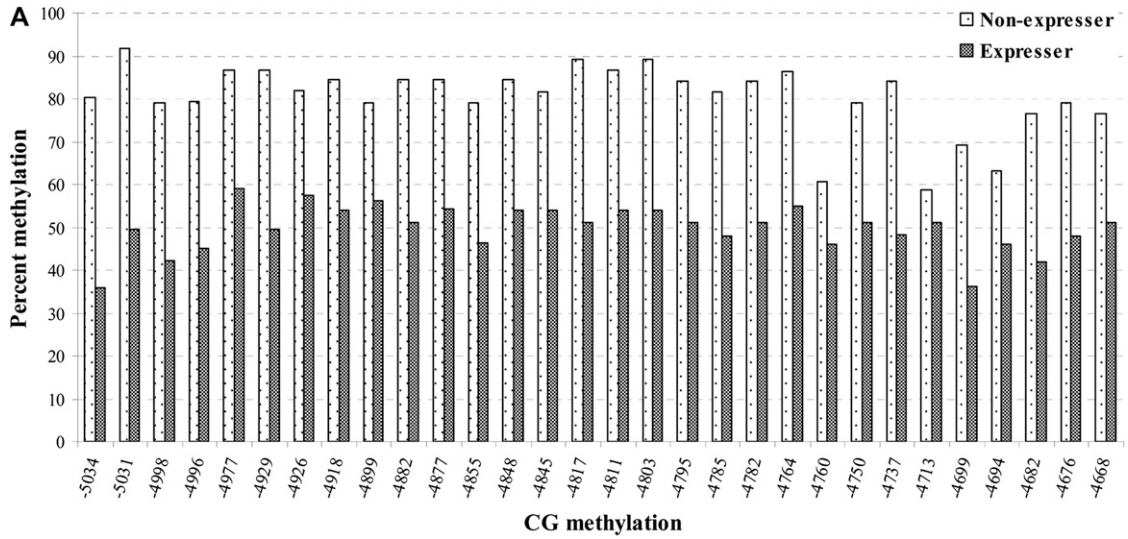

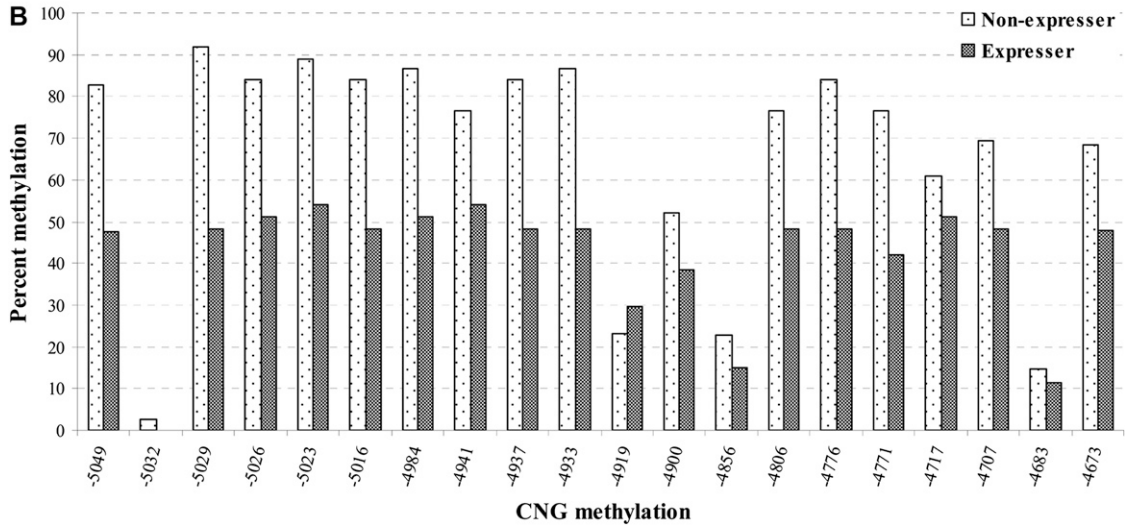

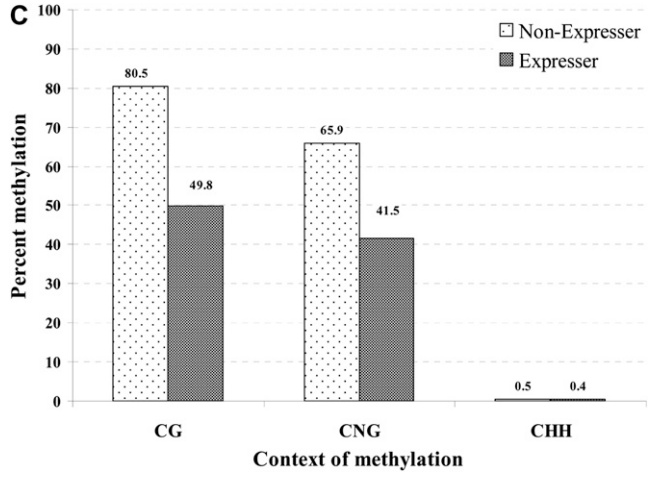

were used, it could not be determined if these insertions were in the same copy of the tandem array. However, a future study might examine if and why certain gene copies are more prone to transposon insertions. Unlike the mutagenesis of *P1-rr* with the *Ac* transposons, the identification of *Mu*-insertion alleles in *P1-wr* did not result in any loss-of-function phenotypes. An obvious explanation for this result would be that more than one

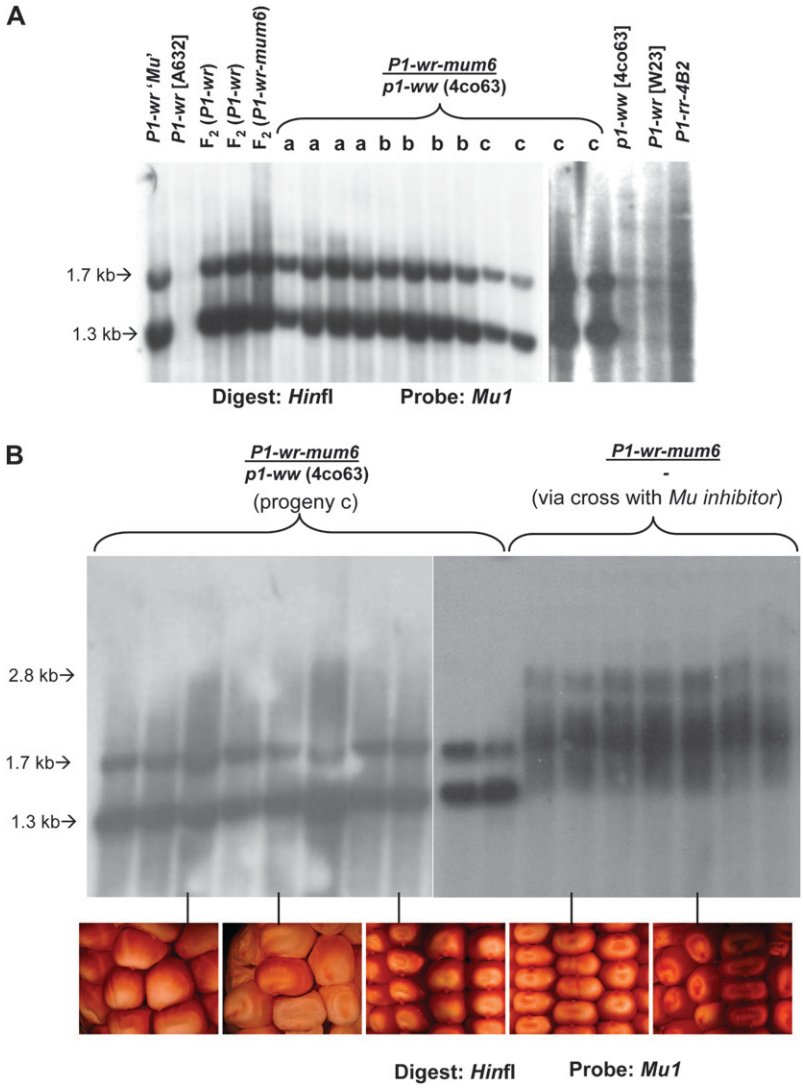

FIGURE 7.—The gain of pericarp function associated with *P1-wr-mum6* does not depend on the *Mu* activity. (A) A DNA gel blot containing *Hin*fI-digested leaf genomic DNA was hybridized with a *Mu1* probe. The 1.3- and 1.7-kb *Hin*fI fragments (marked by arrows on the left) are indicative of active *Mu1* elements. Genotypes studied are indicated at the top. These include the *P1-wr* parental sources used in the TUSC screen to generate *P1-wr-mum6*, F_2 generation *P1-wr* and *P1-wr-mum6* individuals that had colorless pericarp, and *P1-wr-mum6/p1-ww* [4co63] individuals derived from testcross progenies a, b, and c (Figure 3). These testcross progenies are shown by letters a, b, and c, respectively. The *Mu*-active source used to generate *P1-wr-mum6* is denoted by *P1-wr* '*Mu*'. (B) DNA gel blot showing silencing of *Mu* activity in *P1-wr-mum6/p1-ww* by *Mu inhibitor*. DNA of *P1-wr-mum6/−* individuals derived from a cross of *P1-wr-mum6* with *Mu inhibitor* (see MATERIALS AND METHODS) was digested with *Hin*fI and the resulting blot was hybridized with a *Mu1* probe. Arrows to the left of the blots denote the locations of specific bands discussed in the text. Ear photos corresponding to given lanes are shown below the gel.

of the six copies of *P1-wr* are transcribed. Thus, the interruption of a single copy may not have a large net affect on the overall gene expression.

P1-wr-mum6 was characterized because it was the only insertion allele in which a phenotype difference was identified. We specifically investigated how ectopic pericarp pigmentation arose subsequent to a transposon insertion in the 5′-UTR. However, the specific copy of the *P1-wr* multicopy complex in which the *Mu1* insertion resides remains unknown at this point. We showed that the *P1-wr-mum6* phenotype was initially weakly penetrant and was observed as thin red stripes and small sectors on the pericarp. These results suggested that the pericarp pigmentation in *P1-wr-mum6* was induced somatically until it was stably inherited germinally through a clonal sector that affected both the pericarp and the embryo tissue. After this germinal inheritance, uniformly pigmented ears were frequently observed. However, the persistence of variable or "mottled" pericarp pigmentation suggests that *P1-wr-mum6* expression is often affected by somatic changes. On the basis of these observations, we strongly suggest that the presence of *Mu1* in *P1-wr-mum6* lifted a suppression mechanism that otherwise renders *P1-wr* pericarp colorless.

Since the *Mu1* insertion in *P1-wr-mum6* is in the 5′-UTR, it could have directed the expression of the copy in which it resides as is the case with most *Mu*-suppressible alleles in maize (CUI *et al.* 2003). However, we did not detect the presence of such ectopic transcripts. Previous studies indicated that alternate transcript initiation sites are associated with the inactivity of the *MuDR* transposase (BARKAN and MARTIENSSEN 1991; CUI *et al.* 2003). However, we showed that the presence of pigmentation in *P1-wr-mum6* does not depend on the DNA methylation at *Mu1* or the activity of the MuDR transposase protein. Therefore, these experiments suggest that *P1-wr-mum6* expression in pericarp is controlled by a mechanism that is distinct from that functioning in *Mu*-suppressible alleles in maize.

We considered the possibility that the *Mu1* element in *P1-wr-mum6* may affect its expression by physically in-

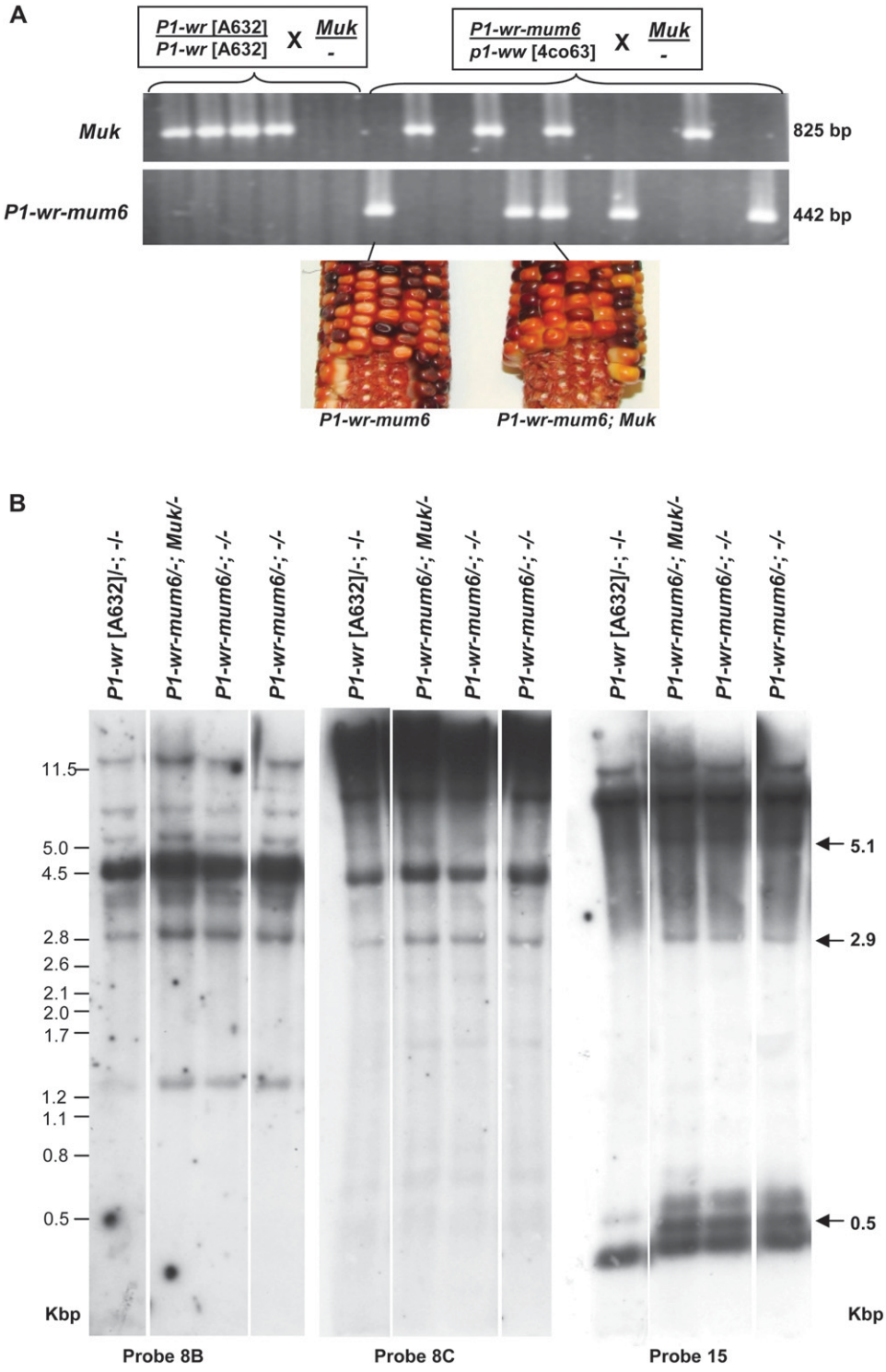

FIGURE 8.—The presence of *Muk* does not affect the DNA methylation of the distal enhancer and intron 2 regions of *P1-wr-mum6*. (A) Ethidium bromide-stained gel picture showing PCR-based genotyping of *Muk* and *P1-wr-mum6* individuals. *P1-wr* [A632] and *P1-wr-mum6/ p1-ww* [4co63] were crossed with a heterozygous *Muk* stock to obtain sibling plants with either active or inactive *Mu* elements. The size of the PCR products is shown on the right. *P1-wr-mum6* ears that contain and lack *Muk* are shown below the gel. (B) DNA gel blot showing the effect of *Muk* on *p1* methylation. A gel blot carrying *Hpa*II-digested DNA of selected genotypes was sequentially hybridized with intron 2-specific probes 8B and 8C and the distal enhancer probe 15. Position and sizes (in kilobase pairs) of bands specific to *P1-wr-mum6* are indicated with arrows on the right. Sizes of the molecular weight markers in kilobase pairs are shown on the left.

terfering with a *cis*-regulatory region that affects the local chromatin structure. In Drosophila, *Gypsy* retrotransposons have been implicated as insulators in such chromatin alterations that disrupt the signaling between enhancers, silencers, and promoters (KUHN and GEYER 2003; KUHN *et al.* 2003; PARNELL *et al.* 2006). In this regard, the *Mu1* insertion in the 5′-UTR of *P1-wr-mum6* might have affected the signaling between upstream regulatory and promoter elements. In fact, we found that *P1-wr-mum6* individuals with stably expressing pericarp pigmentation have undergone hypomethylation at a floral organ-specific distal enhancer element This enhancer previously was shown to be considerably less methylated in *P1-rr* as compared with *P1-wr* (CHOPRA *et al.* 1998). Moreover, the presence of the epigenetic modifier *Ufo1* reduces the DNA methylation at this enhancer, resulting in an increase in pericarp pigmentation (CHOPRA *et al.* 2003). In a parallel study from

mouse, the hypomethylation of a distal enhancer element was required for the long-range (1.2-kb) activation of a downstream promoter (Forrester *et al.* 1999). The role of hypomethylation in distal enhancer function is putatively important because eukaryotic DNA sequences in heterochromatin do not communicate well *in vivo* over distances >1.5 kb (Bondarenko *et al.* 2003).

Bisulfite sequencing analysis revealed that *P1-wr-mum6* expressers were hypomethylated at both CG and CNG sites, indicating that there was a nonselective reduction in DNA methylation. In other words, a specific class of DNA methyltransferase was not specifically inhibited (Chan *et al.* 2005). Rather, the perturbation of chromatin packaging, which is important for maintaining all contexts of DNA methylation, may have led to the gain of function in *P1-wr-mum6* pericarps (Brzeski and Jerzmanowski 2004). The CHH methylation is a useful molecular marker in that it reports the involvement RNA-directed DNA methylation (RdDM). Hence, on the basis of the low CHH methylation levels observed, we conclude that RdDM is not required to maintain DNA methylation levels at the distal enhancer of *P1-wr-mum6*.

Conceivably, hypomethylation at the interrupted copy could spread to uninterrupted copies. The position of the distal enhancer in the interrupted copy is 4.9 kb upstream of the *Mu1* insertion site. The distal enhancer of the interrupted copy would be 1 kb from the 3′ end of an upstream gene copy unless it is the most 5′ copy in the tandem array. If such a spread in DNA hypomethylation/euchromatin occurred, it could explain why the increased RNA expression in *P1-wr-mum6* originates from the uninterrupted (wild-type) copy (or copies). Therefore, it is a distinct possibility that the hypomethylation present at the distal enhancer also affected the uninterrupted copy (or copies) of *P1-wr-mum6* and led to their increased expression in pericarp. Such distal control through chromatin modification is not unprecedented. For instance, paramutation-based silencing of the anthocyanin regulatory *booster1* (*b1*) gene of *Zea mays* is directed by 853-bp tandem repeats of a distal enhancer sequence, which is located ~100 kb upstream of the transcription start site (Stam *et al.* 2002b). These tandem repeats also correlated with a higher order of chromatin packaging (Stam *et al.* 2002a). Because *P1-wr* is multicopy, it may be silenced in pericarp tissue by DNA–DNA interactions between copies that strengthen heterochromatin (Assaad *et al.* 1993; Bender 1998). In other words, the *Mu1* insertion may have disrupted a critical region of a single copy that is important for copy-to-copy associations that rely on heterochromatinization. An example of this phenomenon comes from a fluorescent chromatin-tagging experiment in *Arabidopsis thaliana* that shows that two copies of a transgene separated by 4.2 Mbp can preferentially associate (Watanabe *et al.* 2005). In another example from *Drosophila melanogaster*, the physical pairing and silencing of tandemly repeated *white* (eye color) transgene copies is dependent on both a greater number of tandem repeats and their placement near heterochromatin (Gubb *et al.* 1990; Dorer and Henikoff 1994; Duncan 2002). The variegated eye-color phenotype was an example of position-effect variegation (PEV) in which the normally euchromatic state of the *white* gene is juxtaposed with the heterochromatic state (Dubinin 1936; Spofford 1961). In this regard, *P1-wr-mum6* ears that show mosaicism and kernel-to-kernel differences or sectors may be the result of the juxtaposition between euchromatin and heterochromatin. Therefore, it is conceivable that the presence of tandemly repeated *p1* gene copies facilitates chromatin-based gene silencing.

The interrupted copy in *P1-wr-mum6* may have been accessed by such chromatin-remodeling factors on the basis of an optimal location in the tandem gene array. Alternatively, there may be subtle sequence polymorphisms in the interrupted copy that contribute to the low expression levels in *P1-wr* pericarp. Such a copy might be uniquely recognized by chromatin-remodeling factors. Sequences from complete single copies of *P1-wr* are currently available from the inbred lines W23 (accession no. EF165349; Sekhon *et al.* 2007) and B73 (MAGI database; Fu *et al.* 2005). There are several SNPs that distinguish these *P1-wr* copies of B73 and W23. The *p1* sequences adjacent to the *Mu1* insertion in *P1-wr-mum6* have SNPs that resemble the W23 copy and others that resemble the B73 sequence (accession nos. EU137661 and EU137662, respectively, denote the sequences flanking the 5′ and 3′ ends of *Mu1* in *P1-wr-mum6*). In addition, there were other putative SNPs that were not found in either sequence. Recent evidence also suggests that there are subtle sequence polymorphisms between *P1-wr* [W23] gene copies (P.-H. Wang, R. Sekhon and S. Chopra, personal communication). Functional characterization of these copies should be highly useful in understanding how tandem repeats may regulate tissue-specific expression patterns.

We are grateful to Thomas Peterson, Iowa State University, for his advice regarding the screening of the *Mu*-insertion alleles. We also acknowledge John Snyder and Catherine Svabek for their assistance with DNA isolation and field-based data collection. We thank the anonymous reviewers for their suggested changes to improve the manuscript. This research was performed under a grant from the Hatch project (no. 4154) and supported by National Science Foundation award 0619330 to S.C.

LITERATURE CITED

Anderson, E. G., 1924 Pericarp studies in maize: II. The allelomorphism of a series of factors for pericarp color. Genetics **9:** 442–453.

Assaad, F. F., K. L. Tucker and E. R. Signer, 1993 Epigenetic repeat-induced gene silencing (RIGS) in Arabidopsis. Plant Mol. Biol. **22:** 1067–1085.

Athma, P., and T. Peterson, 1991 Ac induces homologous recombination at the maize P locus. Genetics **128:** 163–173.

Athma, P., E. Grotewold and T. Peterson, 1992 Insertional mutagenesis of the maize P gene by intragenic transposition of Ac. Genetics **131:** 199–209.

Barkan, A., and R. A. Martienssen, 1991 Inactivation of maize transposon Mu suppresses a mutant phenotype by activating an outward-reading promoter near the end of Mu1. Proc. Natl. Acad. Sci. USA **88:** 3502–3506.

Barker, R. F., D. V. Thompson, D. R. Talbot, J. Swanson and J. L. Bennetzen, 1984 Nucleotide sequence of the maize transposable element Mul. Nucleic Acids Res. **12:** 5955–5967.

Bender, J., 1998 Cytosine methylation of repeated sequences in eukaryotes: the role of DNA pairing. Trends Biochem. Sci. **23:** 252–256.

Blanc, G., K. Hokamp and K. H. Wolfe, 2003 A recent polyploidy superimposed on older large-scale duplications in the Arabidopsis genome. Genome Res. **13:** 137–144.

Bondarenko, V. A., Y. V. Liu, Y. I. Jiang and V. M. Studitsky, 2003 Communication over a large distance: enhancers and insulators. Biochem. Cell Biol. **81:** 241–251.

Brink, R. A., and E. D. Styles, 1966 A collection of pericarp factors. Maize Genet. Coop. News Lett. **40:** 149–160.

Brzeski, J., and A. Jerzmanowski, 2004 Plant chromatin–epigenetics linked to ATP-dependent remodeling and architectural proteins. FEBS Lett. **567:** 15–19.

Chan, S. W., I. R. Henderson and S. E. Jacobsen, 2005 Gardening the genome: DNA methylation in Arabidopsis thaliana. Nat. Rev. Genet. **6:** 351–360.

Chandler, V. L., and V. Walbot, 1986 DNA modification of a maize transposable element correlates with loss of activity. Proc. Natl. Acad. Sci. USA **83:** 1767–1771.

Chopra, S., P. Athma and T. Peterson, 1996 Alleles of the maize P gene with distinct tissue specificities encode Myb-homologous proteins with C-terminal replacements. Plant Cell **8:** 1149–1158.

Chopra, S., P. Athma, X. G. Li and T. Peterson, 1998 A maize Myb homolog is encoded by a multicopy gene complex. Mol. Gen. Genet. **260:** 372–380.

Chopra, S., S. M. Cocciolone, S. Bushman, V. Sangar, M. D. McMullen *et al.*, 2003 The maize *Unstable factor for orange1* is a dominant epigenetic modifier of a tissue specifically silent allele of *pericarp color1*. Genetics **163:** 1135–1146.

Cocciolone, S. M., S. Chopra, S. A. Flint-Garcia, M. D. McMullen and T. Peterson, 2001 Tissue-specific patterns of a maize Myb transcription factor are epigenetically regulated. Plant J. **27:** 467–478.

Cui, X., A. P. Hsia, F. Liu, D. A. Ashlock, R. P. Wise *et al.*, 2003 Alternative transcription initiation sites and polyadenylation sites are recruited during Mu suppression at the rf2a locus of maize. Genetics **163:** 685–698.

Das, O. P., and J. Messing, 1994 Variegated phenotype and developmental methylation changes of a maize allele originating from epimutation. Genetics **136:** 1121–1141.

Dietrich, C. R., F. Cui, M. L. Packila, J. Li, D. A. Ashlock *et al.*, 2002 Maize Mu transposons are targeted to the 5′ untranslated region of the gl8 gene and sequences flanking Mu target-site duplications exhibit nonrandom nucleotide composition throughout the genome. Genetics **160:** 697–716.

Dorer, D. R., and S. Henikoff, 1994 Expansions of transgene repeats cause heterochromatin formation and gene silencing in Drosophila. Cell **77:** 993–1002.

Dubinin, N. P., 1936 A new type of position effect. Biol. Zh. **5:** 851–874.

Duncan, I. W., 2002 Transvection effects in Drosophila. Annu. Rev. Genet. **36:** 521–556.

Ferrari, S., D. Vairo, F. M. Ausubel, F. Cervone and G. De Lorenzo, 2003 Tandemly duplicated Arabidopsis genes that encode polygalacturonase-inhibiting proteins are regulated coordinately by different signal transduction pathways in response to fungal infection. Plant Cell **15:** 93–106.

Forrester, W. C., L. A. Fernandez and R. Grosschedl, 1999 Nuclear matrix attachment regions antagonize methylation-dependent repression of long-range enhancer-promoter interactions. Genes Dev. **13:** 3003–3014.

Fu, Y., S. J. Emrich, L. Guo, T. J. Wen, D. A. Ashlock *et al.*, 2005 Quality assessment of maize assembled genomic islands (MAGIs) and large-scale experimental verification of predicted genes. Proc. Natl. Acad. Sci. USA **102:** 12282–12287.

Girard, L., and M. Freeling, 2000 Mutator-suppressible alleles of rough sheath1 and liguleless3 in maize reveal multiple mechanisms for suppression. Genetics **154:** 437–446.

Greene, B., R. Walko and S. Hake, 1994 Mutator insertions in an intron of the maize knotted1 gene result in dominant suppressible mutations. Genetics **138:** 1275–1285.

Grotewold, E., P. Athma and T. Peterson, 1991a Alternatively spliced products of the maize *P* gene encode proteins with homology to the DNA-binding domain of myb-like transcription factors. Proc. Natl. Acad. Sci. USA **88:** 4587–4591.

Grotewold, E., P. Athma and T. Peterson, 1991b A possible hot spot for *Ac* insertion in the maize *P* gene. Mol. Gen. Genet. **230:** 329–331.

Grotewold, E., B. J. Drummond, B. Bowen and T. Peterson, 1994 The myb-homologous *P* gene controls phlobaphene pigmentation in maize floral organs by directly activating a flavonoid biosynthetic gene subset. Cell **76:** 543–553.

Gubb, D., M. Ashburner, J. Roote and T. Davis, 1990 A novel transvection phenomenon affecting the white gene of *Drosophila melanogaster*. Genetics **126:** 167–176.

Hulbert, S. H., and J. L. Bennetzen, 1991 Recombination at the Rp1 locus of maize. Mol. Gen. Genet. **226:** 377–382.

Jacobsen, S. E., H. Sakai, E. J. Finnegan, X. Cao and E. M. Meyerowitz, 2000 Ectopic hypermethylation of flower-specific genes in Arabidopsis. Curr. Biol. **10:** 179–186.

Kliebenstein, D. J., J. Kroymann, P. Brown, A. Figuth, D. Pedersen *et al.*, 2001 Genetic control of natural variation in Arabidopsis glucosinolate accumulation. Plant Physiol. **126:** 811–825.

Kreuzaler, F., and K. Hahlbrock, 1975 Enzymic synthesis of an aromatic ring from acetate units. Partial purification and some properties of flavanone synthase from cell-suspension cultures of Petroselinum hortense. Eur. J. Biochem. **56:** 205–213.

Kuhn, E. J., and P. K. Geyer, 2003 Genomic insulators: connecting properties to mechanism. Curr. Opin. Cell Biol. **15:** 259–265.

Kuhn, E. J., M. M. Viering, K. M. Rhodes and P. K. Geyer, 2003 A test of insulator interactions in Drosophila. EMBO J. **22:** 2463–2471.

Lechelt, C., T. Peterson, A. Laird, J. Chen, S. L. Dellaporta *et al.*, 1989 Isolation and molecular analysis of the maize P locus. Mol. Gen. Genet. **219:** 225–234.

Lippman, Z., A. V. Gendrel, M. Black, M. W. Vaughn, N. Dedhia *et al.*, 2004 Role of transposable elements in heterochromatin and epigenetic control. Nature **430:** 471–476.

Lisch, D., 2002 Mutator transposons. Trends Plant Sci. **7:** 498–504.

Lisch, D., P. Chomet and M. Freeling, 1995 Genetic characterization of the Mutator system in maize: behavior and regulation of Mu transposons in a minimal line. Genetics **139:** 1777–1796.

Lowe, B., J. Mathern and S. Hake, 1992 Active Mutator elements suppress the knotted phenotype and increase recombination at the Kn1-O tandem duplication. Genetics **132:** 813–822.

Lund, G., O. P. Das and J. Messing, 1995 Tissue specific DNase I–sensitive sites of the maize P gene and their changes upon epimutation. Plant J. **7:** 797–807.

Maere, S., S. De Bodt, J. Raes, T. Casneuf, M. Van Montagu *et al.*, 2005 Modeling gene and genome duplications in eukaryotes. Proc. Natl. Acad. Sci. USA **102:** 5454–5459.

Martienssen, R., and A. Baron, 1994 Coordinate suppression of mutations caused by Robertson's mutator transposons in maize. Genetics **136:** 1157–1170.

Martienssen, R., A. Barkan, W. C. Taylor and M. Freeling, 1990 Somatically heritable switches in the DNA modification of Mu transposable elements monitored with a suppressible mutant in maize. Genes Dev. **4:** 331–343.

May, B. P., H. Liu, E. Vollbrecht, L. Senior, P. D. Rabinowicz *et al.*, 2003 Maize-targeted mutagenesis: a knockout resource for maize. Proc. Natl. Acad. Sci. USA **100:** 11541–11546.

Meeley, B., and S. Briggs, 1995 Reverse genetics for maize. Maize Genet. Coop. News Lett. **69:** 67–82.

Parnell, T. J., E. J. Kuhn, B. L. Gilmore, C. Helou, M. S. Wold *et al.*, 2006 Identification of genomic sites that bind the Drosophila suppressor of Hairy-wing insulator protein. Mol. Cell. Biol. **26:** 5983–5993.

Paz-Ares, J., U. Wienand, P. A. Peterson and H. Saedler, 1986 Molecular cloning of the c locus of Zea mays: a locus regulating the anthocyanin pathway. EMBO J. **5:** 829–833.

Piffanelli, P., L. Ramsay, R. Waugh, A. Benabdelmouna, A. D'Hont *et al.*, 2004 A barley cultivation-associated polymorphism conveys resistance to powdery mildew. Nature **430:** 887–891.

Rizzon, C., L. Ponger and B. S. Gaut, 2006 Striking similarities in the genomic distribution of tandemly arrayed genes in Arabidopsis and rice. PLoS Comput. Biol. **2:** e115.

Saghai-Maroof, M. A., K. M. Soliman, R. A. Jorgensen and R. W. Allard, 1984 Ribosomal DNA spacer-length polymorphisms in barley: Mendelian inheritance, chromosomal location, and population dynamics. Proc. Natl. Acad. Sci. USA **81:** 8014–8018.

Sekhon, R. S., T. Peterson and S. Chopra, 2007 Epigenetic modifications of distinct sequences of the p1 regulatory gene specify tissue-specific expression patterns in maize. Genetics **175:** 1059–1070.

Sidorenko, L. V., X. Li, S. M. Cocciolone, S. Chopra, L. Tagliani *et al.*, 2000 Complex structure of a maize Myb gene promoter: functional analysis in transgenic plants. Plant J. **22:** 471–482.

Slotkin, R. K., M. Freeling and D. Lisch, 2003 Mu killer causes the heritable inactivation of the Mutator family of transposable elements in *Zea mays*. Genetics **165:** 781–797.

Slotkin, R. K., M. Freeling and D. Lisch, 2005 Heritable transposon silencing initiated by a naturally occurring transposon inverted duplication. Nat. Genet. **37:** 641–644.

Smith, L. G., B. Greene, B. Veit and S. Hake, 1992 A dominant mutation in the maize homeobox gene, Knotted-1, causes its ectopic expression in leaf cells with altered fates. Development **116:** 21–30.

Spofford, J. B., 1961 Parental control of position-effect variegation. II. Effect of sex of parent contributing white-mottled rearrangement in *Drosophila melanogaster*. Genetics **46:** 1151–1167.

Stam, M., C. Belele, J. E. Dorweiler and V. L. Chandler, 2002a Differential chromatin structure within a tandem array 100 kb upstream of the maize b1 locus is associated with paramutation. Genes Dev. **16:** 1906–1918.

Stam, M., C. Belele, W. Ramakrishna, J. E. Dorweiler, J. L. Bennetzen *et al.*, 2002b The regulatory regions required for B′ paramutation and expression are located far upstream of the maize b1 transcribed sequences. Genetics **162:** 917–930.

Stupar, R. M., K. A. Beaubien, W. Jin, J. Song, M. K. Lee *et al.*, 2006 Structural diversity and differential transcription of the patatin multicopy gene family during potato tuber development. Genetics **172:** 1263–1275.

Veit, B., E. Vollbrecht, J. Mathern and S. Hake, 1990 A tandem duplication causes the Kn1-O allele of Knotted, a dominant morphological mutant of maize. Genetics **125:** 623–631.

Verwoerd, T. C., B. M. Dekker and A. Hoekema, 1989 A small-scale procedure for the rapid isolation of plant RNAs. Nucleic Acids Res. **17:** 2362.

Vollbrecht, E., B. Veit, N. Sinha and S. Hake, 1991 The developmental gene Knotted-1 is a member of a maize homeobox gene family. Nature **350:** 241–243.

Watanabe, K., A. Pecinka, A. Meister, I. Schubert and E. Lam, 2005 DNA hypomethylation reduces homologous pairing of inserted tandem repeat arrays in somatic nuclei of Arabidopsis thaliana. Plant J. **44:** 531–540.

Zhang, F., and T. Peterson, 2005a Comparisons of maize pericarp color1 alleles reveal paralogous gene recombination and an organ-specific enhancer region. Plant Cell **17:** 903–914.

Zhang, J., and T. Peterson, 2005b A segmental deletion series generated by sister-chromatid transposition of Ac transposable elements in maize. Genetics **171:** 333–344.

Communicating editor: A. H. Paterson